HTLV-1 Tax transgenic mice develop spontaneous osteolytic bone metastases prevented by osteoclast inhibition

Ling Gao, Hongju Deng, Haibo Zhao, Angela Hirbe, John Harding, Lee Ratner, and Katherine Weilbaecher

One in 20 carriers of human T-cell leukemia virus type 1 (HTLV-1) will develop adult T-cell leukemia/lymphoma (ATL), a disease frequently associated with hypercalcemia, bone destruction, and a fatal course refractory to current therapies. Overexpression of the HTLV-1–encoded Tax oncoprotein under the human granzyme B promoter causes large granular lymphocytic leukemia/lymphomas in mice. We found that Tax$^+$ mice spontaneously developed hypercalcemia, high-frequency osteolytic bone metastases, and enhanced osteoclast activity. We evaluated Tax tumors for the production of osteoclast-activating factors. Purification of Tax$^+$ tumor cells and nonmalignant tumor-infiltrating lymphocytes demonstrated that each of these populations expressed transcripts for distinct osteoclast-activating factors. We then evaluated the effect of osteoclast inhibition on tumor formation. Mice doubly transgenic for Tax and the osteoclast inhibitory factor, osteoprotegerin, were protected from osteolytic bone disease and developed fewer soft-tissue tumors. Likewise, osteoclast inhibition with bone-targeted zoledronic acid protected Tax$^+$ mice from bone and soft-tissue tumors and prolonged survival. Tax$^+$ mice represent the first animal model of high-penetrance spontaneous osteolytic bone metastasis and underscore the critical role of nonmalignant host cells recruited by tumor cells in the process of cancer progression and metastasis. (Blood. 2005;106:4294-4302)

Introduction

Adult T-cell leukemia/lymphoma (ATL) is an aggressive lymphoproliferative malignancy of helper T lymphocytes and is associated with hypercalcemia and osteolytic bone lesions.[1] Human T-cell leukemia virus type 1 (HTLV-1), the first pathogenic retrovirus discovered in humans, is the etiologic agent of tropical spastic paraparesis myelopathy and ATL.[2,3] It is estimated that 10 to 20 million people worldwide are infected with HTLV-1. Infection with HTLV-1 in infancy is a major risk factor for the development of leukemia.[4] Approximately 1 in 20 people infected with HTLV-1 develop ATL at 20 to 60 years of age, indicating a long latency for this disease. The viral regulatory protein, Tax, has been implicated in the pathogenesis of ATL.[5-7] Tax is a transcriptional activator that can transactivate several viral and cellular genes encoding proteins such as interleukins 6 and 1 (IL-6 and IL-1), tumor necrosis factor α (TNFα), transforming growth factor-β (TGFβ), and parathyroid hormone-related peptide (PTHrP).[8,9] Tax is an oncoprotein with a capacity to transform cells, inhibit p53, and induce tumor formation in several transgenic mouse models using different tissue-specific promoters driving Tax expression.[10-15] Tax expression in mice under the HTLV-1 long terminal repeat or the metallothionein promoter did not produce leukemia; however, increased osteoclast resorption was noted.[15-17] Only the Tax transgenic mice under the regulation of the human granzyme B promoter (expressed in activated T and natural killer [NK] cells) develop lymphoproliferative disease (leukemia, lymphomas, splenomegaly) similar to ATL. Tax$^+$ mice predominantly develop the large granular leukemia/lymphoma (LGL) phenotype rather than the CD4$^+$ lymphoma/leukemia most commonly seen in ATL.[18] Furthermore, Tax$^+$ mice have been used to define cooperating genes critical to lymphoproliferative disease development in ATL.[19-21]

Bone invasion and osteolysis, features of bone metastases, commonly occur in the setting of advanced solid tumors, such as breast, prostate, and lung cancers, but are less common in hematologic malignancies.[22] However, patients with HTLV-1–induced ATL and multiple myeloma (MM) are predisposed to the development of tumor-induced osteolysis and hypercalcemia.[23] One of the striking features of ATL- and MM-induced bone disease is that the bone lesions are predominantly osteolytic with little associated osteoblastic activity. In patients with ATL, elevated serum levels of IL-1, TGFβ, PTHrP, macrophage inflammatory protein (MIP-1α), and receptor activator of nuclear factor-κB ligand (RANKL) have been associated with hypercalcemia.[24-28] Immunodeficient mice that received implants with leukemic cells from patients with ATL or with HTLV-1–infected lymphocytes[29,30] developed hypercalcemia and elevated serum levels of PTHrP.

Tumor-associated destruction of bone is mediated by activated osteoclasts.[22,31] In the bone marrow environment, a variety of tumors have been shown to express factors that directly and/or indirectly stimulate osteoclast differentiation and activity, such as macrophage colony-stimulating factor (M-CSF), IL-1, IL-6, TGFβ,

From the Department of Medicine, Division of Oncology, Washington University School of Medicine, St Louis; the Department of Cellular Biology and Physiology, Division of Oncology, Washington University School of Medicine, St Louis; and the Department of Pathology and Immunology, Washington University School of Medicine, St Louis, MO.

Submitted May 9, 2005; accepted August 4, 2005. Prepublished online as *Blood* First Edition Paper, August 23, 2005; DOI 10.1182/blood-2005-04-1730.

Supported by National Institutes of Health/National Cancer Institute (NIH/NCI) grants, an NIH program project grant (CA100730) administered by Dr Michael Lairmore at The Ohio State University, Pfizer/Washington University Biomedical Research grant, and an Edward G. Mallinckrodt Jr Foundation grant.

The online version of the article contains a data supplement.

Reprints: Katherine Weilbaecher, Washington University School of Medicine, 660 S Euclid Ave, Box 8069, St Louis, MO 63110; e-mail: kweilbae@im.wustl.edu.

The publication costs of this article were defrayed in part by page charge payment. Therefore, and solely to indicate this fact, this article is hereby marked "advertisement" in accordance with 18 U.S.C. section 1734.

TNFα, MIP-1α, RANKL, and PTHrP.[32] In animal models of bone metastasis using tumor cell lines, direct osteoclast inhibition or blockade of PTHrP production by tumor cell lines results in impaired bone invasion and local tumor growth.[33-36] Tumor-cell proliferation in the bone marrow is enhanced by growth factors released on osteoclast resorption of the bone matrix, including TGFβ, insulin-like growth factors (IGFs), and bone morphogenic proteins.[31]

The most widely used animal models of bone metastases use specialized tumor cell lines that are inoculated into the left cardiac ventricle.[35,37,38] Transgenic animal models of spontaneous tumors that metastasize and invade into bone have been reported, yet the incidence of invasive osteolytic bone metastasis is rare (< 1%).[39-41] Spontaneous murine myeloma that recapitulates the disease in humans develops in aged C57BL/KaLwRij mice, but only with a frequency of 0.5%.[42]

Here, we demonstrate that expression of the HTLV-1 viral oncogene Tax in mice was sufficient to cause not only the development of spontaneous lymphoma and leukemia but also sufficient to cause hypercalcemia and vertebral osteolytic bone metastases. Purification of Tax^+ tumor cells and nonmalignant tumor-infiltrating lymphocytes demonstrated that each of these populations expressed distinct osteoclast-activating factors. Osteoclast inhibition through transgenic expression of osteoprotegerin or bisphosphonate therapy prior to the development of leukemia inhibited Tax bone lesions and altered leukemia progression. Thus, Tax^+ mice represent the first animal model of high-penetrance spontaneous osteolytic bone invasion and demonstrate the critical role of nonmalignant host cells recruited by tumor cells in the process of tumor progression and metastasis.

Materials and methods

Animals

Transgenic mice expressing HTLV-1 Tax under the human granzyme B promoter (Tax^+ C57B6/SJL)[18] and transgenic mice expressing osteoprotegerin (OPG^{Tg}) under the apolipoprotein E (ApoE) promoter have been previously described.[43] OPG^{Tg} (C57B6/129) mice were generously provided by Dr Simonet (Amgen, Thousand Oaks, CA). Tax^+OPG^{Tg} and Tax^+OPG^{WT} double transgenic mice were generated by crossing Tax^+ and OPG^{Tg} mice. Genotypes were determined by means of polymerase chain reaction (PCR) on mouse tail genomic DNA. Mice were housed under pathogen-free conditions according to the guidelines of the Division of Comparative Medicine, Washington University School of Medicine. Progress of tumor development was monitored twice a week, and animals were humanely killed at the end of the experiment or if tumors grew larger than 20 mm in diameter. The animal studies committee institutional review board of Washington University School of Medicine approved all experiments. Zoledronic acid, generously provided by Dr Jonathan Green of Novartis, Basel, Switzerland, was administered at a dose of 0.75 μg per mouse per week (approximately 30 μg/kg).

Radiographs and dual-energy x-ray absorptiometry (DEXA)

Animals were radiographed in the prone position and exposed to 20 KVP for 15 seconds using an x-ray System (Faxitron, Buffalo Grove, IL). Osteolytic lesions were defined as areas of increased radiolucency disrupting bone marrow contour and invading into bone cortex. Isolated femurs, tibias, and tails bone mineral density (BMD) were measured and analyzed by a PIXImus2 scanner (Lunar Corporation, Madison, WI).

Bone histology

Mouse bones were fixed in formalin, decalcified in 14% EDTA (ethylenediaminetetraacetic acid), paraffin embedded and stained with hematoxylin and eosin and for TRAP (tartrate-resistant acid phosphatase). Images were visualized under a Nikon Eclipse TE300 microscope equipped with a Plan Fluor 20×/0.45 objective lens (Nikon, Tokyo, Japan) and a Magnafire camera (Optronics, Goleta, CA). Trabecular bone area was measured according to a standard protocol using the Osteomeasure Analysis System (Osteometrics, Decatur GA).[44]

Osteoclast functional assays

Whole bone marrow extracted from Tax^+ and wild-type littermate mice was plated at a concentration of 5×10^4 cells per well in a 48-well plate with 5 replicates. Cells were refed every other day with α-MEM (Minimum Essential Media) with 10% fetal calf serum (FCS) in M-CSF (12 ng/mL) and glutathione *S*-transferase (GST)–RANKL (10 ng/mL and 30 ng/mL) and incubated at 37°C in 6% CO_2, 94% air for 5 days and were fixed in 3% paraformaldehyde and TRAP stained (Sigma, St Louis, MO). A quantitative TRAP solution assay was performed by adding a colorimetric substrate, 5.5 mM *P*-nitrophenyl phosphate at day 5 in addition to the presence of 10 mM sodium tartrate at pH 4.5. The reaction product was quantified by measuring optic absorbance at 405 nm.[45]

Flow cytometry and immunofluorescent staining

Single-cell suspensions were prepared from peripheral soft-tissue tumors. Samples were depleted of red blood cells. Cells were labeled with fluorescein isothiocyanate (FITC)–conjugated rat anti–mouse CD16/32 (FcγR II/III; Pharmingen, La Jolla, CA) monoclonal antibody according to the manufacturer's recommendations. Cells were placed on slides, fixed in cold methanol, and stained with Wright-Giemsa-Grünwald (Sigma) or prepared for further immunostaining and incubated with primary anti-Tax monoclonal antibody (1:1000; AIDS Reagent Program, Rockville, MD), washed, and then incubated with FITC-labeled secondary antibody goat anti-rabbit (1:100; Vector Laboratory, Burlingame, CA). Enzyme-linked immunosorbent assay (ELISA) quantification of IL-6 serum levels was performed using ELISA kit from R&D Systems (Minneapolis, MN) according to manufacturer's instructions.

Reverse transcription–PCR and real-time PCR

Mouse preosteoblast line ST-2 (gift from Dr Teitelbaum) was cultured in α-MEM with 10% FCS. Total RNA from ST-2 cells and primary tumor populations were isolated with the RNeasy kit (QIAGEN, Valencia, CA) and digested with deoxyribonuclease to eliminate genomic DNA. cDNA was made using Superscript first-strand synthesis system for RT-PCR (Invitrogen, Carlsbad, CA). RT-PCRs were performed with mouse gene-specific primers at 25, 30, and 35 cycles: RANKL, RANK, OPG, TGFβ1, TNFα, IL-1α, and IL-1β were from R&D System (IL-6 sense, TGGAGTCACAGAAGGAGTGGCTAAG, and antisense, TCTGACCACAGTGAGGA-ATGTCCAC; M-CSF sense, GACTTCATGCCAGATTGCC, and antisense, GGTGGC-TTTAGGGTACA GG; glyceraldehyde-3-phosphate dehydrogenase [GAPDH] sense, ACTTTGTCAAGCTCATTTCC, and antisense, TGCAGCGAACTTTATTGATG). Real-time PCR primers for IL-6, RANKL, and GAPDH were purchased from Applied Biosystems (Foster City, CA), and reactions were carried out in triplicate on an ABI PRISM 7700 Sequence Detector System (ABI, Foster City, CA) as previously described.[46]

Retroviral transduction

The Tax oncogene was cloned into a modified mouse stem-cell virus (MSCV) driving green fluorescent protein (GFP) separated by an internal ribosomal entry site whose sequence was previously described.[47] Replication-defective retrovirus was produced with the MSCV-Tax-GFP construct with Ecopac (Cell Genesys, Foster City, CA) into 293T cells by using Superfect reagent (Qiagen, Chatsworth, CA). Retrovirus was subsequently collected in the conditioned medium. ST-2 cells were seeded at 1.5×10^4 cells per well in 6-well plates with α-MEM, 20% FCS for 48 hours and transduced with MSCV-Tax retroviral stock with polybrene (4 μg/mL) for 24 hours. Total RNAs were collected 3 days after infection.

Statistical analysis

Group mean values were compared by 2-tailed student *t* test or as otherwise indicated.

Results

Tax+ transgenic mice develop spontaneous osteolytic bone metastases and hypercalcemia

Tax+ mice develop large granular leukemia/lymphomas on the tails, legs, and ears that also invade liver, spleen, and lung between the ages of 4 and 12 months.[18] Clinically, human ATL can be associated with osteolytic lesions and hypercalcemia. Therefore, skeletal x-ray images were obtained on Tax+ mice as they developed external peripheral tumors. Between the ages of 3 and 12 months, 86% of Tax+ mice that developed soft-tissue tumors (32 of 37) had radiographic evidence of osteolytic bone destruction (Figure 1A; Table 1). Radiographically evident osteolytic lesions were often observed in the absence of overlying soft-tissue tumors. The serum levels of calcium (Ca^{2+}) in tumor-bearing Tax+ mice were significantly higher than in age-matched wild-type mice ($P < .01$; Figure 1B). Serum calcium levels in 1-month-old preleukemic Tax mice and age-matched wild-type mice were not elevated (data not shown).

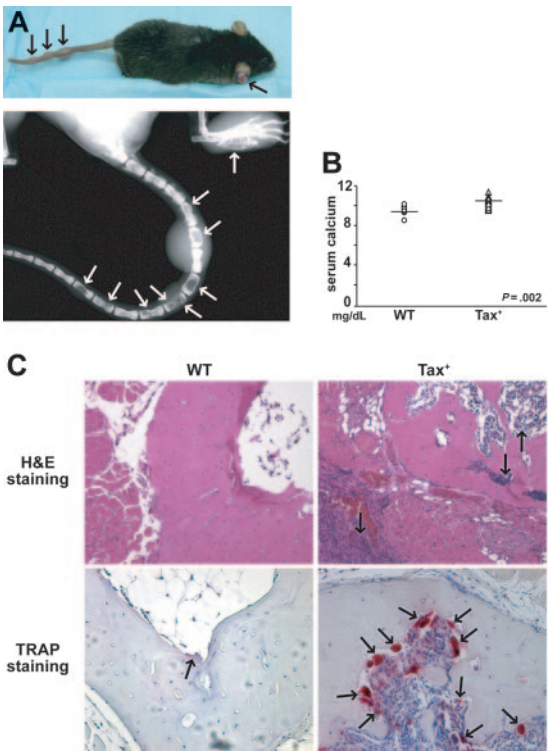

Figure 1. Tax+ mice develop osteolytic bone lesions and hypercalcemia of malignancy. (A) Between the ages of 4 and 12 months, Tax+ mice develop large granular leukemia/lymphoma tumors on the tails, legs, and ears (black arrows). Radiographic imaging demonstrates osteolytic bone destruction (white arrows) in the tail vertebra and the feet of a Tax+ mouse. (B) Dot plot of serum calcium (Ca^{2+}) levels of tumor-bearing Tax+ mice (n = 19) and wild-type age-matched controls (n = 8). Tax+ mice had significantly higher serum Ca^{2+} ($P < .01$). (C) Tartrate-resistant acid phosphatase (TRAP) staining on decalcified tail vertebra of a representative Tax+ mouse. Hematoxylin-eosin staining shows tumor cells in the bone marrow, cortical bone, and subcutaneous tissue of a Tax+ mouse as indicated by arrows (top, × 20). TRAP stain of decalcified tail vertebra shows increased osteoclast recruitment at the marrow bone interface (bottom, × 20).

Table 1. Incidence of bone metastasis in Tax+ mice with tumors

Radiographic analysis	1-6 mo, % (n)	7-12 mo, % (n)
Bone lesions	81 (13)	86 (32)
No bone lesions	19 (3)	13 (5)

Osteoclast recruitment and bone mineral loss are associated with Tax tumor development

Histologic analysis of vertebral bones from leukemic Tax+ mice demonstrated tumor cells invading the bone marrow space and cortical bone (Figure 1C). Staining for osteoclast-specific TRAP demonstrated increased numbers of osteoclasts at the interface of bone and bone marrow in Tax+ bones (Figure 1C).

To assess bone physiology in Tax+ mice BMD measurements of preleukemic (1 month of age) and leukemic (mice developed peripheral tumors) Tax+ mice were obtained by DEXA conducted on isolated tail, femoral, and tibial bones. Body weights were not significantly different among 1-, 2-, and 3-month-old Tax+ and wild-type littermates (data not shown). No significant difference in tail vertebral, femoral, or tibial BMD was observed between 1-month-old preleukemic Tax+ and wild-type littermate controls (Figure 2A). In contrast, significant decreases in the tail vertebral, femoral, and tibial BMD were obtained in tumor-bearing Tax+ mice compared with age-matched controls ($P < .05$; Figure 2B). Thus, diffuse osteolysis developed coincidentally with tumor progression as mice aged.

Preleukemic Tax+ mice have normal osteoclast function and leukemic Tax+ mice have enhanced osteoclast formation

Tumor-associated bone destruction is mediated primarily by the augmentation of bone resorption, either through increased osteoclast recruitment or enhanced osteoclast function.[31] We sought to determine whether Tax+ mice had abnormal bone physiology prior to the development of tumors. Using an ex vivo assay that reflects potentiation of osteoclastogenesis in vivo,[48] osteoclast formation was evaluated in Tax+ mice and wild-type littermates before and after tumor development. Whole bone marrow (WBM) cells from 1-month-old preleukemic Tax+ mice and age-matched wild-type mice were cultured in low dose of M-CSF (12 ng/mL) and GST-RANKL (10 ng/mL and 30 ng/mL) to induce osteoclast differentiation. Osteoclasts (OCs) from WBM of Tax+ mice developed into multinucleated TRAP+ OCs at a similar rate compared with wild-type mice (Figure 2C-D). In contrast, WBM from 7-month-old tumor-bearing Tax+ mice produced significantly more osteoclasts compared with age-matched wild-type mice, demonstrating enhanced osteoclast formation potential in leukemic Tax+ mice ($P < .05$; Figure 2E-F). Osteoclasts cultured from bone marrow macrophages from preleukemic Tax+ and wild-type littermates functioned normally in quantitative TRAP activity assays (Figure S1A, available at the *Blood* website; see the Supplemental Figures link at the top of the online article) and acid-induced calcium phosphate resorption (data not shown). Granzyme B expression as a surrogate for Tax transgene expression was not detected in osteoclasts from Tax+ mice. Murine NK cells serve as a positive control (Figure S1B). Finally, histomorphometric analysis of femoral and tibial bones from 1-month-old preleukemic Tax+ mice demonstrated normal osteoclast numbers on the bone surface as compared with wild-type littermates (Figure S1C). Thus no obvious differences between preleukemic (mice aged 1 month) Tax+ OCs and wild-type littermate OCs in vivo or in vitro were

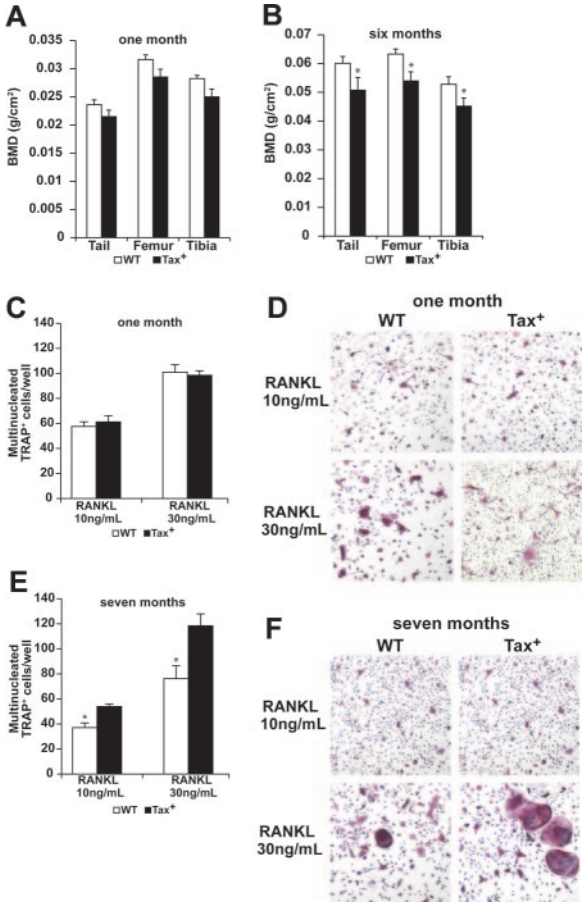

Figure 2. Tumor-bearing Tax mice have decreased bone mineral density and enhanced osteoclastogenesis. (A-B) Bone mineral density (BMD) of Tax$^+$ mice measured by dual-energy x-ray absorptiometry (DEXA) is depicted as the mean ± SEM. One-month-old Tax$^+$ mice have normal BMD on tails, tibias, and femurs as compared with their wild-type littermates ($P > .05$, n = 10). Tumor-bearing Tax$^+$ mice have significantly decreased BMD on tails, tibias, and femurs as compared with the wild-type littermates (*$P < .05$, n = 10). (C) Whole bone marrow cells from a 1-month-old Tax$^+$ mouse and a wild-type littermate were cultured in low-dose M-CSF (12 ng/mL) and GST-RANKL (10 ng/mL and 30 ng/mL) for 5 days; cells were fixed and TRAP stained. Three independent experiments were repeated. Multinucleated TRAP-positive osteoclasts of Tax$^+$ mice and wild-type mice were counted and depicted as the mean ± SEM. There was not a significant difference ($P > .05$), indicating similar osteoclast formation between 1-month-old Tax$^+$ and wild-type mice. (D) Representative TRAP staining of 1-month-old wild-type and Tax$^+$ whole bone marrow–derived osteoclast cultures at day 5 (× 20). (E) Whole bone marrow cells from a 7-month-old Tax$^+$ tumor-bearing mouse and a wild-type littermate cultured under low M-CSF (12 ng/mL) and GST-RANKL (10 ng/mL and 30 ng/mL) for 5 days; cells were fixed and TRAP stained. Three independent experiments were repeated. Multinucleated TRAP-positive osteoclasts of Tax$^+$ mice were more abundant compared with wild-type mice, indicating enhanced osteoclast formation in tumor-bearing Tax$^+$ mice (*$P < .01$). (F) Representative TRAP staining of 7-month-old wild-type and Tax$^+$ whole bone marrow osteoclast cultures at day 5 (× 20).

observed. Therefore, it is unlikely that the increased osteolysis seen in leukemic Tax$^+$ mice was a consequence of intrinsic differences in Tax$^+$ bone cells but rather was related to enhanced osteoclast formation in tumor-bearing mice.

Isolated Tax$^+$ tumor cells and nonmalignant tumor-infiltrating lymphocytes express distinct osteoclastogenic factors

Tax has been shown to transactivate several cellular genes involved in osteoclast development, such as IL-1, IL-6, TNFα, and PTHrP.[10] Tax$^+$ tumors are composed of 25% to 35% Tax-expressing tumor cells as well as associated inflammatory cells and stromal cells. To isolate Tax tumor cells, we prepared single-cell suspensions from fresh Tax$^+$ tail tumors and labeled the cells with FITC-conjugated anti–FcγR II/III (CD16/CD32), a cellular marker for NK cells. Cells with FITC-high, -low, and -negative staining were collected by fluorescence-activated cell sorting (FACS) (Figure 3A) for analysis and histologic evaluation. By Wright-Giemsa-Grünwald staining, LGL Tax$^+$ tumor cells were harbored in the FcγR II/III (CD16/CD32) FITC-high cell population (Figure 3B). FcγR FITC-low cell populations contained predominantly neutrophils, and FITC-negative cell populations contained lymphocytes and stromal cells. Tax was primarily expressed in the FITC-high tumor-cell population and not by the CD16/CD32-negative lymphocyte population as measured by RT-PCR (Figure 3A). Furthermore, immunofluorescent staining for Tax showed that Tax protein was located both in the nucleus and cytoplasm of CD16/CD32 FITC-high cells (Figure 3C), which is consistent with previous reports.[49]

Total RNA was isolated, and cDNA was generated from FITC-high and FITC-negative cells collected by FACS sorting. By RT-PCR, we found that tumor cells expressed transcripts for IL-6, M-CSF, and IL-1α, whereas RANKL, the critical osteoclastogenic factor, was predominantly expressed in the FITC-negative lymphocyte- and stromal-cell population. Both the tumor FITC-high

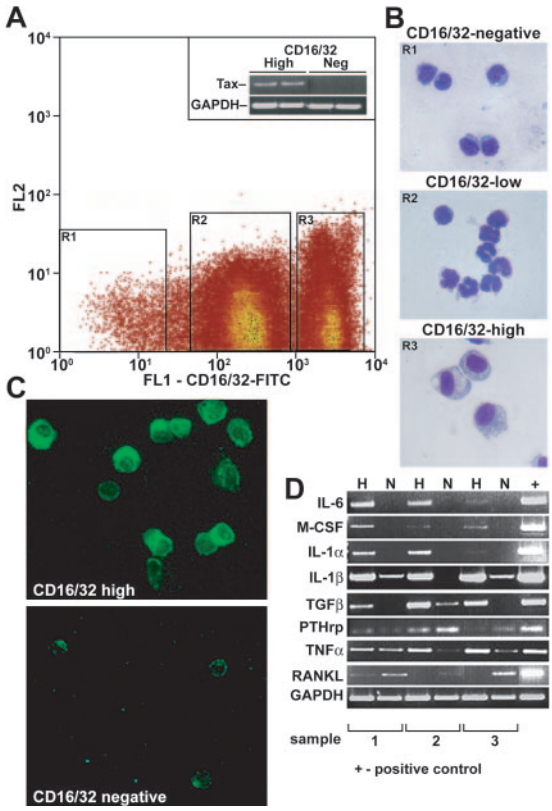

Figure 3. Isolated Tax tumor cells express transcripts for osteoclast-activating factors. (A) Single-cell suspensions of 3 Tax$^+$ tumors were sorted by FACS according to FcγR II/III (CD16/CD32) FITC-negative, -low, and -high intensity. Expression of the *Tax* gene was detected in CD16/CD32-high but not in -negative cell populations by RT-PCR. GAPDH was used as an internal control. (B) Cytospin and Wright-Giemsa-Grünwald staining was performed on sorted cells. CD16/CD32 FITC-negative cells were normal lymphocytes/stromal cells. CD16/CD32 FITC-high cells were tumor cells, whereas CD16/CD32 FITC-low cells were neutrophils (× 20). (C) CD16/CD32 FITC-high cells were immunofluorescently stained with Tax antibody (green, × 20). (D) RT-PCR of selected osteoclast-activating factors in CD16/CD32 FITC-negative (N) and FITC-high (H) cells was performed on the mRNA of purified cell types isolated from whole tumors. RANKL was expressed in CD16/CD32 lymphocytes/stromal cells; IL-6, IL-1α, and M-CSF were expressed in Tax tumor cells; IL-1β, TGFβ, PTHrP, and TNFα were expressed in both CD16/CD32-negative and -high cell populations.

population and the FITC-negative populations expressed transcripts for IL-1β, TNFα, PTHrP, and TGFβ (Figure 3D). CD16/CD32-fractionated bone marrow and spleen cells from a Tax tumor-bearing mouse demonstrated that IL-6 was expressed by the CD16/CD32-high fraction, and RANKL in the CD16/CD32-negative fraction as was seen for the fractionated soft-tissue tumor (data not shown). Interestingly, we also found by RT-PCR that purified Tax tumor cells (CD16/CD32 FITC-high) did not express transcripts for OPG the soluble inhibitor of RANKL but did express transcripts for RANK, the receptor for RANKL (Supplemental Figure S2). Thus, purified Tax-expressing tumor cells expressed transcripts for the osteoclast-activating factors IL-6, M-CSF, IL-1α and IL-1β, TNFα, and TGFβ, whereas nonmalignant, non–Tax-expressing tumor-infiltrating lymphocytes recruited to Tax tumors expressed transcripts for the critical osteoclastogenic factor RANKL.

Tax expression enhances IL-6 expression in vitro and in vivo

By real-time quantitative RT-PCR, IL-6 was expressed by isolated Tax$^+$ tumor cells but not by the FcγR II/III–negative tumor-associated inflammatory cells (Figure 4A). However, RANKL was expressed by the FcγR II/III–negative tumor-associated inflammatory cells but only at low and in some cases undetectable levels by the FcγR II/III–high tumor cells (Figure 4B). It is known that tumor-derived IL-6 plays an important role in multiple myeloma–induced bone destruction,[23] and IL-6 stimulates osteoclast activation.[50] Furthermore, serum IL-6 levels have been shown to be elevated in HTLV-1–positive ATL.[51] We measured the serum levels of soluble IL-6 from Tax$^+$ and wild-type mice by ELISA. As in patients with ATL, serum IL-6 levels were significantly higher ($P < .05$) in tumor-bearing Tax$^+$ mice compared with age-matched wild-type mice (Figure 4E).

IL-6 has also been shown to be a downstream target of Tax in T cells.[52] To confirm that RANKL is not a direct transcription target of Tax, Tax was introduced into a preosteoblast cell line, ST-2,[53] which can produce RANKL on stimulation with osteotrophic factors, such as 1,25-dihydroxy-vitamin D_3 and prostaglandins.[54] ST-2 cells were transduced with a retroviral vector, MSCV-Tax-GFP. As demonstrated in Figure 4C to D, Tax overexpression induced an increase in IL-6 and TNFα but not RANKL expression. M-CSF and TGFβ were constitutively expressed in ST-2 cells regardless of various stimulations, demonstrating the lack of significant toxicity from the MSCV transduction (Figure 4D). These data indicate that Tax$^+$ mice have elevated levels of IL-6 and that Tax expression directly induced IL-6 and TNFα but not RANKL.

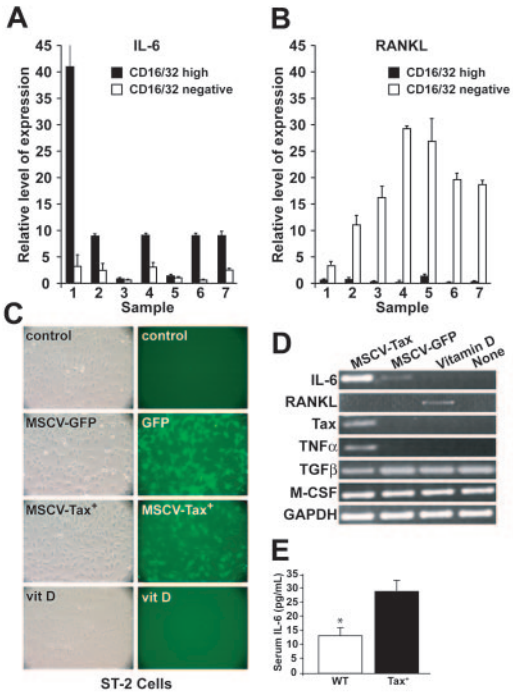

Figure 4. Tax induces IL-6 expression in tumor cells. (A-B) Real-time RT-PCR of IL-6 and RANKL normalized to GAPDH from 7 CD16/CD32-fractionated Tax tumors from 7 mice. RANKL was expressed in normal lymphocytes/stromal cells, whereas IL-6 was expressed in Tax tumor cells. All data are depicted as the mean ± SEM. (C) The preosteoblast cell line ST-2 was transduced with MSCV-Tax-GFP or MSCV-GFP. Controls were nontreated ST-2 cells and ST-2 cells treated with vitamin D for 3 days. Left panel pictures were taken under phase contrast microscopy; right panel pictures were taken under FITC channel of conventional fluorescent microscopy. (D) MSCV-Tax transduction in ST-2 cells induces IL-6 and TNFα expression but not RANKL. RT-PCR of selected osteoclast-activating factors was performed on cDNAs from transduced ST-2 cells, vitamin D–treated ST-2 cells, and nontreated ST-2 cells. (E) Serum was obtained retroorbitally, and IL-6 levels were determined by ELISA. Results for Tax$^+$ (n = 17) and wild-type (n = 19) mice are shown as picogram per milliliter. Tax$^+$ mice have increased serum IL-6 levels ($P < .05$). Values are depicted as the mean ± SEM.

Tax$^+$OPG^{Tg} mice were protected from osteolytic bone lesions and soft tissue tumor development

To determine whether inhibiting osteoclast function would prevent Tax$^+$ tumor-associated bone lesions, Tax$^+$ mice were crossed to the osteoclast-defective OPG^{Tg} mice to produce Tax$^+$OPG^{Tg} mice. Osteoprotegerin is a soluble decoy receptor for RANKL and is normally expressed by osteoblasts and B cells. When murine OPG is constitutively expressed by hepatocytes under the human ApoE promoter, the OPG^{Tg} mice develop osteopetrosis and lack functional and mature osteoclasts.[43] Thus, any osteoclast-activating factors that act through RANKL will be abrogated in OPG^{Tg} mice.

Tax$^+$OPG^{Tg} mice were markedly protected from tumor-associated osteolysis compared with Tax$^+$OPG^{WT} littermates (Figure 5). By 9 months of age, 21% of Tax$^+$OPG^{Tg} mice developed radiographic osteolytic lesions; in contrast, 68% of Tax$^+$OPG^{WT} mice developed multiple osteolytic bone tumors throughout the vertebrae (Table 2). Representative x-rays demonstrate diminished osteolytic lesions and enhanced bone mineral in the Tax$^+$OPG^{Tg} mice compared with Tax$^+$OPG^{WT} mice (Figure 5A). In the mice that developed bone lesions, the numbers of bone lesions were significantly diminished in the Tax$^+$OPG^{Tg} (Figure 5B). Unexpectedly, Tax$^+$OPG^{Tg} mice developed fewer soft-tissue tumors compared with Tax$^+$OPG^{WT} mice ($P < .01$; Figure 5C). Thus, Tax$^+$ mice genetically altered to lack functional osteoclasts were protected from tumor-associated bone destruction consistent with the hypothesis that osteoclasts play a critical role in Tax tumor-associated osteolysis. Likewise, genetic disruption of osteoclast function by overexpression of OPG resulted in impaired leukemia progression manifested by decreased soft tissue tumor production and bone destruction in Tax$^+$OPG^{Tg} mice.

Bisphosphonate treatment not only prevented osteolytic bone destruction but also decreased tumor burden in Tax$^+$ mice

Amino-bisphosphonates are highly effective bone-targeted inhibitors of bone resorption that disrupt osteoclast function and have a skeletal half-life of more than 6 months but a serum half-life of several hours.[55] Amino-bisphosphonates disrupt geranylgeranylation of proteins, impair osteoclast development, and induce mature osteoclast apoptosis.[56] Bisphosphonates are routinely used in

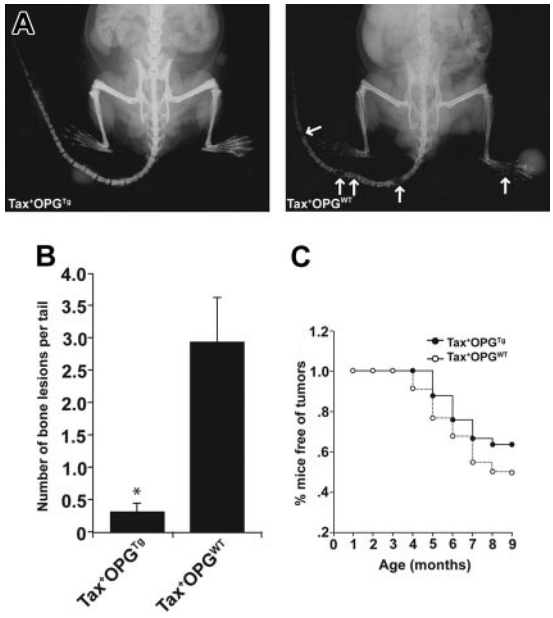

Figure 5. Tax$^+$OPG^{Tg} mice are protected from osteolytic bone lesions and soft tissue tumor development. Tax$^+$ mice were crossed with OPG^{Tg} mice. Tax$^+$OPG^{Tg} mice (n = 33) and Tax$^+$OPG^{WT} (n = 22) littermates were evaluated weekly for peripheral tumor formation, and radiographic images were taken at 3, 6, and 9 months of age. Experiments were ended when mice were 9 months old. (A) Representative radiographic images of a Tax$^+$OPG^{Tg} mouse and a Tax$^+$OPG^{WT} mouse at 9 months of age. Tax$^+$OPG^{WT} mouse demonstrates osteolytic bone lesions on the tail vertebrae (arrows). (B) In mice that developed osteolysis, Tax$^+$OPG^{WT} mice show significantly increased bone lesions on the tail vertebrae ($P < .01$) compared with Tax$^+$OPG^{Tg}. Bone lesion number is depicted as the mean ± SEM. (C) Tax$^+$OPG^{Tg} mice are protected from the development of soft-tissue tumors ($P < .01$, by a paired *t* test in SigmaPlot 2001 version 9; Systat Software, Point Richmond, CA).

patients with cancer with established osteolytic metastasis to decrease tumor-associated bone destruction and to relieve bone pain. It has been observed in some clinical trials that bisphosphonates can improve overall survival in patients with myeloma and breast cancer when administered at early stages of cancer prior to the development of overt bone metastases,[57-62] but the mechanism of this effect on survival is still under investigation.

To test the hypothesis that inhibition of Tax$^+$ tumor-stimulated osteoclast activity could affect the development of overt bone lesions as seen in Tax$^+$OPG^{Tg} mice, zoledronic acid bisphosphonate therapy was administered to preleukemic 1-month-old Tax$^+$ mice before signs of overt lymphoma or tumor-associated osteolysis were evident. Weekly subcutaneous injections of zoledronic acid (n = 17) or saline placebo (n = 12) were administered to randomly assigned 1-month-old Tax$^+$ mice littermates. Mice were evaluated weekly for the development of peripheral tumor formation and x-rayed at 3, 6, and 9 months of age or whenever they developed the first visual peripheral tumors, or at death. The experimental trial was terminated when the Tax$^+$ mice were 9 months of age. Zoledronic acid–treated Tax$^+$ mice were protected from bone metastases as compared with saline-treated Tax$^+$ mice, with 83% of living Tax$^+$ mice treated with saline carrying bone metastases at 9 months compared with 17% of living Tax$^+$ mice

Table 2. Incidence of bone metastasis in Tax$^+$OPG^{Tg} mice according to age

	3 mo, n (%)	6 mo, n (%)	9 mo, n (%)
Tax$^+$OPG^{Tg}	0	3/33 (9)	7/33 (21)
Tax$^+$OPG^{WT}	0	8/22 (36)	15/22 (68)

Table 3. Incidence of bone metastasis in Tax$^+$ mice

	3 mo, n (%)	6 mo, n (%)	9 mo, n (%)
Zoledronic acid	0/15 (0)	1/14 (7)	2/12 (17)
Saline	0/8 (0)	8/9 (89)	5/6 (83)

Tax$^+$ mice were treated with zoledronic acid or saline according to age.

treated with zoledronic acid (Table 3). Representative x-rays demonstrated diminished osteolytic lesions and enhanced bone mineral in the zoledronic acid–treated mice compared with saline-treated mice (Figure 6A). Of the mice that developed bone lesions, the numbers of vertebral body lesions were greatly reduced in zoledronic acid–treated mice (Figure 6B). Zoledronic acid–treated Tax$^+$ mice showed significant decreases in soft tissue tumor development ($P < .01$; Figure 6C). Significantly, zoledronic acid–treated mice had an improved overall survival compared with Tax$^+$ littermate placebo-treated controls ($P < .01$; Figure 6D), with 71% of zoledronic acid–treated Tax$^+$ mice still alive at 9 months compared with 50% of placebo-treated Tax$^+$ mice. We found that early treatment with bisphosphonate zoledronic acid before the development of overt disease prevented not only tumor-associated bone destruction and soft tissue lymphoma development but also increased survival, suggesting that tumor-induced osteoclast activity affects tumor growth and metastatic progression.

Discussion

The HTLV-1 viral oncogene, Tax, has been shown to be critical to the pathogenesis of adult T-cell leukemia (ATL). We demonstrate

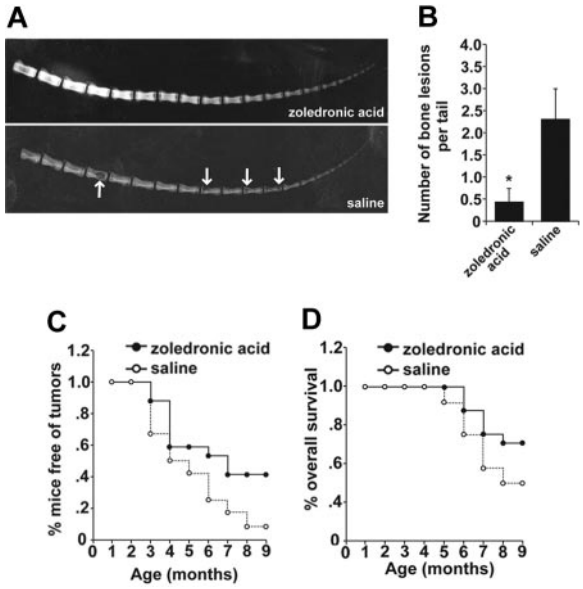

Figure 6. Early bisphosphonate treatment prevents osteolytic bone lesions and enhances overall survival in Tax$^+$ mice. Tax$^+$ littermate mice were randomly divided into zoledronic acid–treated (0.75 μg per mouse subcutaneous injection weekly, n = 17) or saline controls (n = 12) at 1 month of age. Mice were evaluated biweekly for peripheral tumor formation, and radiographic images were taken at 3, 6, and 9 months of age. Experiments were ended when mice were 9 months old. (A) Representative radiographic images of Tax$^+$ mice treated with zoledronic acid or saline at 9 months of age. Tax$^+$ mice treated with saline show overt bone lesions (arrows). (B) Of the mice that developed osteolysis, numbers of tail lesions are significantly higher in saline-treated mice ($P < .05$). Bone lesion number is depicted as the mean ± SEM. (C) Tax$^+$ mice treated with zoledronic acid were protected from the development of peripheral tumors ($P < .01$ by a paired *t* test in SigmaPlot 2001). (D) Tax$^+$ mice treated with zoledronic acid show increased overall survival ($P < .01$ by a paired *t* test in SigmaPlot 2001).

that Tax expression in mice not only caused leukemia but also was sufficient to cause the ATL skeletal manifestations of hypercalcemia, vertebral osteolytic bone metastases, and enhanced osteoclast activity. Tax^+ mice possessed normal bone physiology prior to tumor development. We found that Tax^+ mice spontaneously developed osteolytic bone metastasis (86% incidence) and hypercalcemia in association with the development of soft-tissue lymphomas. Tax^+ mice with bone metastases and soft-tissue tumors had accelerated loss of bone mineral density and had enhanced osteoclast activity compared with age-matched controls. It is unclear whether Tax tumors develop in the lymph nodes and then spread to the bone marrow or vice versa. Studies are under way involving luciferase-expressing tumor cells to identify in real time the sequence of early tumor development in this model. Tax^+ bone tumors cannot be called true metastases, although they model many aspects of bone metastases, including invasion into and associated destruction of cortical bone and multifocal location.

Tax^+ tumors are composed of Tax-expressing tumor cells, tumor-associated inflammatory cells, and stromal cells which express distinct osteoclast-activating factors. Purified Tax^+ tumor cells expressed transcripts for IL-6, a known transcriptional target gene of the Tax protein, in addition to M-CSF, IL-1α, IL-1β, TGFβ, and TNFα, all of which have been shown to activate osteoclast and to enhance tumor-associated bone loss. Interestingly, the nonmalignant tumor-infiltrating lymphocytes recruited to the Tax^+ tumors expressed the critical osteoclast factor, RANKL, which we did not find to be a direct transcriptional target of Tax. Thus, Tax expression in tumor cells resulted in both direct and indirect induction of critical osteoclast-activating factors. Studies from samples from patients with multiple myeloma have demonstrated that malignant plasma cells express a range of cytokines that directly and indirectly activate osteoclastic resorption and suppress osteoblast activity.[23] Tax bone disease closely models myeloma bone disease and could be a useful model to better understand tumor cell/host cell interaction in vivo. Evaluation in Tax^+ tumors of other osteoclast-activating factors that have been implicated in myeloma bone disease such as MIP-1α and Dickkopf-1 (DKK1) is under way.

Generalized bone mineral loss, measured by DEXA, is a common occurrence in patients with multiple myeloma, as well as patients with solid tumor with bone metastasis, and it was seen in our Tax^+ ATL animal model. There was a nonstatistical trend toward decreased BMD seen as early as 1 month of age in the Tax^+ mice. It is possible that Tax^+ mice could be developing tumors as early as 1 month of age that were not yet visibly or radiographically evident and that these early tumors were affecting body mass and bone mineral density. Likewise, metastasis in the vertebral bones, one of the most common sites of bone metastasis in humans, occurred at high frequency in the Tax model. This provides an advantage over other animal models of bone metastasis, such as the intracardiac tumor-cell line injection models, in which the most common site of invasion in is in the growth plates of the tibia and femur, which are less common sites for metastasis in adults.[35,63] One possible explanation for the differences in skeletal distribution of osteolytic lesions observed in the Tax^+ mice is that Tax^+ tumors most commonly develop in adult mice (aged 4-9 months), whereas the intracardiac injection models use young mice aged 6 weeks, with highly vascularized growth plates. Thus, the Tax^+ bone metastasis model represents the first high-frequency animal model of bone metastasis that mirrors what is commonly observed in human bone metastasis.

OPG^{Tg} mice overexpress the RANKL decoy receptor (osteoprotegerin) and have functionally reduced levels of RANKL and impaired osteoclast development. Consistent with the current concept that functional osteoclasts are required in tumor-associated bone destruction, we found that Tax^+OPG^{Tg} mice were protected from osteolytic bone metastases. Unexpectedly, Tax^+OPG^{Tg} mice also developed fewer soft-tissue tumors and thus impaired leukemia tumor progression in this animal model, suggesting a role for osteoclast resorption and bone turnover in the growth and dissemination of Tax^+ tumor cells. We found that purified Tax tumor cells expressed transcripts for the RANK receptor, and it is possible that RANKL, expressed by tumor-infiltrating lymphocytes and by osteoblasts in the bone marrow environment, could provide growth and survival signals to RANK-expressing Tax tumor cells. The potential role of suppression of the RANK-RANKL axis in Tax tumor development is under current investigation. These results indicate that RANKL production either from tumor-infiltrating lymphocytes or in the bone environment likely plays a critical pathogenic role in Tax-induced bone metastasis and tumor development.

The overall incidence of bone and soft-tissue tumors was lower in the mice from the OPG^{Tg} genetic crosses (Figure 5) compared with Tax^+ mice alone (Figure 6). This difference in tumor incidence could reflect differences in modifying genes or innate immunity between the mouse transgenic strains. Rather than compare the Tax^+OPG^{Tg} with the Tax^+ mice from the Tax^+ transgenic colony, we used littermate controls that harbored the Tax transgene but not the OPG transgene, Tax^+OPG^{WT}, to minimize the effect of genetic background.

We then used a pharmacologic approach to block osteoclast function by treating Tax^+ mice with the bone-targeted bisphosphonate, zoledronic acid, at 1 month of age before the development of visible soft-tissue tumors or bone metastases. Zoledronic acid prevented Tax-induced bone metastasis, prevented soft tissue tumor development, and prolonged overall survival. These data indicate that osteoclast inhibition through the RANKL pathway or through use of the bone-targeted bisphosphonates not only blocked bone metastasis but also prevented tumor progression, thus suggesting that host cells recruited by tumor cells play a critical role in tumor biology.

Whether bisphosphonates have direct effects on tumor cells or indirect effects on tumor cells mediated by changes they cause in the bone microenvironment has long been debated. Clinical data indicate that the bisphosphonates have little effect on soft-tissue metastasis if they are administered after metastases are already established.[61,64,65] However, a growing body of evidence in vitro suggests that bisphosphonates have direct effects on tumor cells.[66]

Possible explanations for the improvement in overall survival and decreased tumor burden seen in the bisphosphonate-treated Tax^+ mice could be that bisphosphonates are pure osteoclast inhibitors and disrupt the "vicious cycle" of tumor-induced release of tumor growth factors, such as IGF-1, and TGFβ, liberated from the bone matrix on osteoclast activation. Likewise, our data using the osteoclast defective OPG^{Tg} mice suggest that disruption of osteoclastic resorption through the OPG/RANKL pathway also decreased nonbone disease tumor burden. Thus, two bone-targeted, osteoclast-inhibitory approaches resulted in decreases in bone metastasis and decreases in overall tumor burden and soft tissue tumor development in the Tax^+ transgenic model consistent with the notion that disruption of the osteoclast resorption and formation negatively affects tumor growth and progression. An alternative explanation for the bisphosphonate effect on survival could be a

direct antitumor effect of the bisphosphonate on tumor cells in the bone marrow for which there is in vitro data from other groups.[67] Alternatively, zoledronic acid has been demonstrated to activate gd-T-cells through an indirect mechanism involving inhibition of farnesyl diphosphate (FPP) synthase. Activated γδ T cells could theoretically enhance antitumor immunity and/or alter T-cell–mediated osteoclast cytokine production, thereby providing an additional explanation for decreased tumor burden in zoledronic acid–treated Tax^+ mice. However, this effect of zoledronic acid on γδ T cells has only been shown in primates and is not thought to occur in murine models.[68-72] Our data suggest an overall effect of early bisphosphonate intervention on Tax tumor development in vivo. Evaluation of the effect of bisphosphonates on tumor apoptosis and necrosis in Tax^+ mice is currently under way.

Our data support a causal role for Tax in the development of osteolytic bone destruction in Tax-induced lymphoproliferative disease and the acquisition of the bone phenotype in patients with ATL. Purified Tax^+ tumor cells and tumor-recruited nonmalignant tumor-infiltrating lymphocytes expressed critical osteoclastogenic factors. Despite its critical role in the pathogenesis of ATL, Tax protein expression levels have been reported to be low and at times undetectable from patient ATL cells.[4] The precise role of Tax in leukemia maintenance and progression remains under investigation. Our data demonstrate that Tax was sufficient to induce lymphoproliferative disease and skeletal complications often associated with ATL. Osteoclast inhibition through transgenic expression of the osteoclast inhibitory factor, osteoprotegerin, or bisphosphonate therapy prior to the development of leukemia inhibited Tax-induced bone metastases and diminished leukemia progression. Our results demonstrate the critical role of nonmalignant host cells recruited by tumor cells in the process of cancer progression and metastasis. Tax^+ mice represent the first animal model of high-penetrance spontaneous osteolytic bone metastasis and underscore the critical role of nonmalignant host cells in bone metastasis. Our data demonstrate that intervention with bisphosphonates before the development of overt lymphoma/leukemia prevented tumor-associated osteolysis, dissemination of soft-tissue tumors, and prolonged overall survival, suggesting a role for early bisphosphonate therapy in patients infected with HTLV-1.

Acknowledgments

We are indebted to Drs. Michael Tomasson, Steve Teitelbaum, and Paddy Ross for their support and advice during this project. We thank Dr Scott Simonet from Amgen Pharmaceuticals for the generous gift of the OPG^{Tg} mice. We thank Dr Shibani Mitra-Kaushik for advice regarding Tax^+ mice breeding and care. We thank Dr Jonathan Green for the gift of zoledronic acid and advice regarding drug dosing in these studies. We thank Dr Tsukahara for the gift of the MSCV-Tax-GFP retrovirus. We thank Drs. Lairmore and Bernal-Mizrahi and Elizabeth Morgan for their critical reading of this manuscript. We thank William Eades in the Siteman Cancer Center high-speed sorter core facility (supported in part by P30 CA91842) and the Center for Nutrition Research Unit for assistance with DEXA scanning supported in part by DK56341.

References

1. Ohuchida T, Nishitani H, Kamikawaji N, Niho Y, Ooiwa T, Matsuura K. "Adult T-cell leukemia/lymphoma" with bone demineralization. Skeletal Radiol. 1985;14:194-197.
2. Weber J. HTLV-1 and tropical spastic paraparesis, 2: the human T-cell lymphotropic virus type 1. Trans R Soc Trop Med Hyg. 1989;83:729-731.
3. Yamano Y, Nagai M, Brennan M, et al. Correlation of human T-cell lymphotropic virus type 1 (HTLV-1) mRNA with proviral DNA load, virus-specific CD8(+) T cells, and disease severity in HTLV-1-associated myelopathy (HAM/TSP). Blood. 2002;99:88-94.
4. Ratner L. Adult T cell leukemia lymphoma. Front Biosci. 2004;9:2852-2859.
5. Uchiyama T. Human T cell leukemia virus type I (HTLV-I) and human diseases. Annu Rev Immunol. 1997;15:15-37.
6. Franchini G, Streicher H. Human T-cell leukaemia virus. Baillieres Clin Haematol. 1995;8:131-148.
7. Korber B, Okayama A, Donnelly R, Tachibana N, Essex M. Polymerase chain reaction analysis of defective human T-cell leukemia virus type I proviral genomes in leukemic cells of patients with adult T-cell leukemia. J Virol. 1991;65:5471-5476.
8. Azran I, Schavinsky-Khrapunsky Y, Aboud M. Role of Tax protein in human T-cell leukemia virus type-I leukemogenicity. Retrovirology. 2004;1:20-44.
9. Shuh M, Derse D. Ternary complex factors and cofactors are essential for human T-cell leukemia virus type 1 tax transactivation of the serum response element. J Virol. 2000;74:11394-11397.
10. Grossman WJ, Ratner L. Transgenic mouse models for HTLV-I infection. J Acquir Immune Defic Syndr Hum Retrovirol. 1996;13(suppl 1):S162-S169.
11. Kehn K, Fuente Cde L, Strouss K, et al. The HTLV-I Tax oncoprotein targets the retinoblastoma protein for proteasomal degradation. Oncogene. 2005;24:525-540.
12. Pise-Masison CA, Brady JN. Setting the stage for transformation: HTLV-1 Tax inhibition of p53 function. Front Biosci. 2005;10:919-930.
13. Mahieux R, Pise-Masison CA, Nicot C, Green P, Hall WW, Brady JN. Inactivation of p53 by HTLV type 1 and HTLV type 2 Tax trans-activators. AIDS Res Hum Retroviruses. 2000;16:1677-1681.
14. Nicot C, Mahieux R, Takemoto S, Franchini G. Bcl-X(L) is up-regulated by HTLV-I and HTLV-II in vitro and in ex vivo ATLL samples. Blood. 2000; 96:275-281.
15. Ruddle NH, Li CB, Horne WC, et al. Mice transgenic for HTLV-I LTR-tax exhibit tax expression in bone, skeletal alterations, and high bone turnover. Virology. 1993;197:196-204.
16. Iwakura Y, Tosu M, Yoshida E, et al. Induction of inflammatory arthropathy resembling rheumatoid arthritis in mice transgenic for HTLV-I. Science. 1991;253:1026-1028.
17. Saggioro D, Rosato A, Esposito G, et al. Inflammatory polyarthropathy and bone remodeling in HTLV-I Tax-transgenic mice. J Acquir Immune Defic Syndr Hum Retrovirol. 1997;14:272-280.
18. Grossman WJ, Kimata JT, Wong FH, Zutter M, Ley TJ, Ratner L. Development of leukemia in mice transgenic for the tax gene of human T-cell leukemia virus type I. Proc Natl Acad Sci U S A. 1995;92:1057-1061.
19. Mitra-Kaushik S, Harding JC, Hess JL, Ratner L. Effects of the proteasome inhibitor PS-341 on tumor growth in HTLV-1 Tax transgenic mice and Tax tumor transplants. Blood. 2004;104:802-809.
20. Mitra-Kaushik S, Harding J, Hess J, Schreiber R, Ratner L. Enhanced tumorigenesis in HTLV-1 tax-transgenic mice deficient in interferon-gamma. Blood. 2004;104:3305-3311.
21. Portis T, Grossman WJ, Harding JC, Hess JL, Ratner L. Analysis of p53 inactivation in a human T-cell leukemia virus type 1 Tax transgenic mouse model. J Virol. 2001;75:2185-2193.
22. Mundy GR. Metastasis to bone: causes, consequences and therapeutic opportunities. Nat Rev Cancer. 2002;2:584-593.
23. Roodman GD. Mechanisms of bone lesions in multiple myeloma and lymphoma. Cancer. 1997; 80:1557-1563.
24. Nosaka K, Miyamoto T, Sakai T, Mitsuya H, Suda T, Matsuoka M. Mechanism of hypercalcemia in adult T-cell leukemia: overexpression of receptor activator of nuclear factor kappaB ligand on adult T-cell leukemia cells. Blood. 2002;99:634-640.
25. Okada Y, Tsukada J, Nakano K, Tonai S, Mine S, Tanaka Y. Macrophage inflammatory protein-1alpha induces hypercalcemia in adult T-cell leukemia. J Bone Miner Res. 2004;19:1105-1111.
26. Ishibashi K, Ishitsuka K, Chuman Y, et al. Tumor necrosis factor-beta in the serum of adult T-cell leukemia with hypercalcemia. Blood. 1991;77: 2451-2455.
27. Wano Y, Hattori T, Matsuoka M, et al. Interleukin 1 gene expression in adult T cell leukemia. J Clin Invest. 1987;80:911-916.
28. Watanabe T, Yamaguchi K, Takatsuki K, Osame M, Yoshida M. Constitutive expression of parathyroid hormone-related protein gene in human T cell leukemia virus type 1 (HTLV-1) carriers and adult T cell leukemia patients that can be transactivated by HTLV-1 tax gene. J Exp Med. 1990; 172:759-765.
29. Liu Y, Dole K, Stanley JR, et al. Engraftment and tumorigenesis of HTLV-1 transformed T cell lines in SCID/bg and NOD/SCID mice. Leuk Res. 2002;26:561-567.
30. Imada K, Takaori-Kondo A, Sawada H, et al. Serial transplantation of adult T cell leukemia cells into severe combined immunodeficient mice. Jpn J Cancer Res. 1996;87:887-892.

31. Roodman GD. Mechanisms of bone metastasis. N Engl J Med. 2004;350:1655-1664.
32. Choong PF. The molecular basis of skeletal metastases. Clin Orthop. 2003:S19-S31.
33. Gallwitz WE, Guise TA, Mundy GR. Guanosine nucleotides inhibit different syndromes of PTHrP excess caused by human cancers in vivo. J Clin Invest. 2002;110:1559-1572.
34. Yin JJ, Selander K, Chirgwin JM, et al. TGF-beta signaling blockade inhibits PTHrP secretion by breast cancer cells and bone metastases development. J Clin Invest. 1999;103:197-206.
35. Guise TA, Yin JJ, Taylor SD, et al. Evidence for a causal role of parathyroid hormone-related protein in the pathogenesis of human breast cancer-mediated osteolysis. J Clin Invest. 1996;98:1544-1549.
36. Kang Y, Siegel PM, Shu W, et al. A multigenic program mediating breast cancer metastasis to bone. Cancer Cell. 2003;3:537-549.
37. Yoneda T, Michigami T, Yi B, Williams PJ, Niewolna M, Hiraga T. Actions of bisphosphonate on bone metastasis in animal models of breast carcinoma. Cancer. 2000;88:2979-2988.
38. Arguello F, Baggs RB, Frantz CN. A murine model of experimental metastasis to bone and bone marrow. Cancer Res. 1988;48:6876-6881.
39. Rosol TJ, Tannehill-Gregg SH, LeRoy BE, Mandl S, Contag CH. Animal models of bone metastasis. Cancer. 2003;97:748-757.
40. Winter SF, Cooper AB, Greenberg NM. Models of metastatic prostate cancer: a transgenic perspective. Prostate Cancer Prostatic Dis. 2003;6:204-211.
41. Klezovitch O, Chevillet J, Mirosevich J, Roberts RL, Matusik RJ, Vasioukhin V. Hepsin promotes prostate cancer progression and metastasis. Cancer Cell. 2004;6:185-195.
42. Radl J, Croese JW, Zurcher C, Van den Enden-Vieveen MH, de Leeuw AM. Animal model of human disease: multiple myeloma. Am J Pathol. 1988;132:593-597.
43. Simonet WS, Lacey DL, Dunstan CR, et al. Osteoprotegerin: a novel secreted protein involved in the regulation of bone density. Cell. 1997;89:309-319.
44. Parfitt AM. Bone histomorphometry: standardization of nomenclature, symbols, and units. Report of the ASBMR histomorphometry of nomenclature committee. J Bone Miner Res. 1987;2:595-610.
45. Lam J, Takeshita S, Barker JE, Kanagawa O, Ross FP, Teitelbaum SL. TNF-alpha induces osteoclastogenesis by direct stimulation of macrophages exposed to permissive levels of RANK ligand. J Clin Invest. 2000;106:1481-1488.
46. Yu J, Marsh S, Ahluwalia R, McLeod HL. Ferredoxin reductase: pharmacogenomic assessment in colorectal cancer. Cancer Res. 2003;63:6170-6173.
47. Grisolano JL, O'Neal J, Cain J, Tomasson MH. An activated receptor tyrosine kinase, TEL/PDGFbetaR, cooperates with AML1/ETO to induce acute myeloid leukemia in mice. Proc Natl Acad Sci U S A. 2003;100:9506-9511.
48. Lane NE, Yao W, Nakamura MC, et al. Mice lacking the integrin beta5 subunit have accelerated osteoclast maturation and increased activity in the estrogen-deficient state. J Bone Miner Res. 2005;20:58-66.
49. Bex F, Gaynor RB. Regulation of gene expression by HTLV-I Tax protein. Methods. 1998;16:83-94.
50. Sohara Y, Shimada H, Minkin C, Erdreich-Epstein A, Nolta JA, DeClerck YA. Bone marrow mesenchymal stem cells provide an alternate pathway of osteoclast activation and bone destruction by cancer cells. Cancer Res. 2005;65:1129-1135.
51. Anzai S, Takayasu S, Fujiwara S, Tateyama M, Taira H, Takashita M. Elevation of IL-6 in ATL patient with a pathological fracture. J Dermatol. 2002;29:644-647.
52. Mori N, Shirakawa F, Shimizu H, et al. Transcriptional regulation of the human interleukin-6 gene promoter in human T-cell leukemia virus type I-infected T-cell lines: evidence for the involvement of NF-kappa B. Blood. 1994;84:2904-2911.
53. Udagawa N, Takahashi N, Akatsu T, et al. The bone marrow-derived stromal cell lines MC3T3-G2/PA6 and ST2 support osteoclast-like cell differentiation in cocultures with mouse spleen cells. Endocrinology. 1989;125:1805-1813.
54. Kitazawa R, Kitazawa S. Vitamin D(3) augments osteoclastogenesis via vitamin D-responsive element of mouse RANKL gene promoter. Biochem Biophys Res Commun. 2002;290:650-655.
55. Reszka AA, Rodan GA. Bisphosphonate mechanism of action. Curr Rheumatol Rep. 2003;5:65-74.
56. Rogers MJ, Gordon S, Benford HL, et al. Cellular and molecular mechanisms of action of bisphosphonates. Cancer. 2000;88:2961-2978.
57. Croucher PI, De Hendrik R, Perry MJ, et al. Zoledronic acid treatment of 5T2MM-bearing mice inhibits the development of myeloma bone disease: evidence for decreased osteolysis, tumor burden and angiogenesis, and increased survival. J Bone Miner Res. 2003;18:482-492.
58. Berenson JR, Lichtenstein A, Porter L, et al. Long-term pamidronate treatment of advanced multiple myeloma patients reduces skeletal events. Myeloma Aredia Study Group. J Clin Oncol. 1998;16:593-602.
59. Cameron D. Proven efficacy of zoledronic acid in the treatment of bone metastases in patients with breast cancer and other malignancies. Breast. 2003;12(suppl 2):S22-S29.
60. Diel IJ, Kaufmann M, Costa SD, et al. Micrometastatic breast cancer cells in bone marrow at primary surgery: prognostic value in comparison with nodal status. J Natl Cancer Inst. 1996;88:1652-1658.
61. Hortobagyi GN, Theriault RL, Porter L, et al. Efficacy of pamidronate in reducing skeletal complications in patients with breast cancer and lytic bone metastases. Protocol 19 Aredia Breast Cancer Study Group. N Engl J Med. 1996;335:1785-1791.
62. Powles T, Paterson S, Kanis JA, et al. Randomized, placebo-controlled trial of clodronate in patients with primary operable breast cancer. J Clin Oncol. 2002;20:3219-3224.
63. Arguello F. Metastasis to bone and bone marrow. Cancer Res. 1988;48:6876-6881.
64. Saad F. Treatment of bone complications in advanced prostate cancer: rationale for bisphosphonate use and results of a phase III trial with zoledronic acid. Semin Oncol. 2002;29:19-27.
65. Lipton A, Theriault RL, Hortobagyi GN, et al. Pamidronate prevents skeletal complications and is effective palliative treatment in women with breast carcinoma and osteolytic bone metastases: long term follow-up of two randomized, placebo-controlled trials. Cancer. 2000;88:1082-1090.
66. Santini D, Vespasiani Gentilucci U, Vincenzi B, et al. The antineoplastic role of bisphosphonates: from basic research to clinical evidence. Ann Oncol. 2003;14:1468-1476.
67. Cheng YY, Huang L, Lee KM, Xu JK, Zheng MH, Kumta SM. Bisphosphonates induce apoptosis of stromal tumor cells in giant cell tumor of bone. Calcif Tissue Int. 2004;75:71-77.
68. Mariani S, Muraro M, Pantaleoni F, et al. Effector gammadelta T cells and tumor cells as immune targets of zoledronic acid in multiple myeloma. Leukemia. 2005;19:664-670.
69. Rischer M, Pscherer S, Duwe S, Vormoor J, Jurgens H, Rossig C. Human gammadelta T cells as mediators of chimaeric-receptor redirected anti-tumour immunity. Br J Haematol. 2004;126:583-592.
70. Gober HJ, Kistowska M, Angman L, Jeno P, Mori L, De Libero G. Human T cell receptor gammadelta cells recognize endogenous mevalonate metabolites in tumor cells. J Exp Med. 2003;197:163-168.
71. Wilhelm M, Kunzmann V, Eckstein S, et al. Gammadelta T cells for immune therapy of patients with lymphoid malignancies. Blood. 2003;102:200-206.
72. Thompson K, Rogers MJ. Statins prevent bisphosphonate-induced gamma, delta-T-cell proliferation and activation in vitro. J Bone Miner Res. 2004;19:278-288.